

Thermodynamic Studies of the Core Histones: Ionic Strength and pH Dependence of H2A–H2B Dimer Stability[†]

Vassiliki Karantza, Andreas D. Baxevanis,[‡] Ernesto Freire, and Evangelos N. Moudrianakis*

Department of Biology, The Johns Hopkins University, Baltimore, Maryland 21218

Received January 11, 1995; Revised Manuscript Received February 20, 1995[§]

ABSTRACT: The thermal stability of the core histone dimer H2A–H2B has been studied by high-sensitivity differential scanning calorimetry and circular dichroism spectroscopy. The unfolding transition temperature of the 28 kDa H2A–H2B dimer increases as a function of both the ionic strength of the solvent and the total protein concentration. At neutral pH and physiological ionic strength, the thermal denaturation is centered at about 50 °C with a corresponding enthalpy change of about 40 kcal/mol of 14 kDa monomer unit and an excess heat capacity of about 1.4 kcal/(K·mol) of 14 kDa monomer unit. The H2A–H2B dimer is stable mainly between pH 5.5 and 10.5. Below pH 4.0, the system is unfolded at all temperatures. The thermodynamic analysis is performed at low ionic strength where almost complete reversibility is attained, since higher salt conditions seem to promote aggregation and irreversibility of the transitions. Analysis of the data shows that at low ionic strength and pH values between 6.5 and 8.5, the H2A–H2B dimer behaves as a highly cooperative system, melting as a single unit without any detectable intermediates of dissociated, yet folded, H2A and H2B monomers. This is consistent with the observed protein concentration dependence of the midpoint of the thermal denaturation. The two-state unfolding process can be described by the general scheme $AB \rightarrow 2U$, indicating that the individual H2A and H2B polypeptides are folded, stable entities only when complexed as the H2A–H2B dimer and that the major contribution to the stabilization of the dimer derives from the coupling between the H2A and H2B interfaces.

Since the original proposal of a fundamental repeating protein–DNA unit in chromatin (Kornberg, 1974), studies on the thermal denaturation of the structural components of chromatin have centered around the association of the histone octamer with the DNA in core nucleosomes. Most of these studies have characterized these associations through changes in the hyperchromicity of the DNA component and by monitoring the circular dichroism of both DNA and protein components as a function of temperature. Several studies have also utilized differential scanning calorimetry (DSC),¹ which provides a direct measure of the energetics of the system in question [*cf.* Freire et al. (1990) for a recent review of DSC].

Weischet et al. (1979) observed that core particles exhibit a two-step optical transition (60–65 and 73 °C) and that these hyperchromic shifts at 260 nm are paralleled by two calorimetric melting transitions at the same temperatures. These changes were preceded by changes in the circular

dichroism spectra at 273 nm, indicative of structural rearrangements of DNA toward that of free DNA; the second calorimetric and hyperchromic transition occurred concomitantly with a loss of histone secondary structure as monitored by CD at 223 nm. Bina et al. (1980) compared native nucleosomes at low ionic strength, a state where the nucleosome is partially unfolded and expanded, with nucleosomes in which the histones had been cross-linked by dimethyl suberimidate, yielding a more compact structure at low ionic strength. The enthalpy values obtained by melting both of these nucleosome preparations were similar, suggesting that the enthalpy change for the low ionic strength unfolding transition is small. Olins et al. (1977) had previously examined nucleosomes in low ionic strength solvents in the presence of varying amounts of urea and found that, despite the thermal stabilization of DNA when complexed with histones, urea could destabilize all histone–DNA interactions. Simpson (1979) examined the sedimentation behavior of nucleosomes as well as changes in the CD signal as a function of temperature. A low-temperature “transition” was observed at 34 °C, and this was interpreted to represent the partial extension of the DNA from the core and not a denaturation event. S1 nuclease ³⁵S-labeling experiments demonstrated that slight heating of the nucleosomes (below the aforementioned thermal transition) led to the freeing of 20 bp of DNA at either end of the nucleosome, with the central core still intact. Finally, Poon and Seligy (1980) performed electron microscopic studies on core nucleosomes at different temperatures and observed a major structural rearrangement around 70 °C, paralleling the second thermal transition previously discussed (Weischet et al., 1979). The electron micrographs indicated that nucleo-

[†] Publication No. 1498 from the Department of Biology, The Johns Hopkins University. This research was supported in part by a grant from the National Institutes of Health (RR-04328).

* To whom correspondence should be addressed.

[‡] Present address: National Center for Biotechnology Information, National Institutes of Health, Bethesda, MD 20894.

[§] Abstract published in *Advance ACS Abstracts*, April 1, 1995.

¹ Abbreviations: ΔC_p , observed difference in the heat capacity between the unfolded and the native states; ΔH , enthalpy change; ΔH_{cal} , calorimetric enthalpy change; ΔS , entropy change; $[\Theta]_d$, molar ellipticity, in degrees centimeter squared per decimole; CD, circular dichroism; CM-cellulose, (carboxymethyl)cellulose; DSC, differential scanning calorimetry; EDTA, ethylenediaminetetraacetic acid; HEPES, *N*-(2-hydroxyethyl)piperazine-*N'*-2-ethanesulfonic acid; kDa, kilodalton(s); MES, 2-(*N*-morpholino)ethanesulfonic acid; NaDodSO₄, sodium dodecyl sulfate; PMSF, phenylmethanesulfonyl fluoride; % rev, percent reversibility; SSR, sum of the squared residuals of the fit; T_m , melting temperature.

somes were changing from compact to open, ringlike structures.

Based on the findings of these and other studies, van Holde (1989) postulated the following sequence for the events taking place during the thermal denaturation of the core nucleosome. At low temperatures, the core particle is comprised of two each of the four core histones around which 146 bp DNA is wrapped; both the histones and the DNA are in their native forms. At 34–40 °C, 20 bp DNA is released from either end of the nucleosome, but the DNA retains its double-stranded character. At 60–65 °C, the DNA tails previously released from the core begin to denature, assuming a more single-stranded character. Finally, by 75–80 °C, all of the DNA has separated into single strands, and the core histones have lost all of their secondary structure, existing as extended polypeptides.

While the thermodynamic behavior of the components of the nucleosome has been partially characterized, only Benedict et al. (1984) have reported on the behavior of the core histones in the absence of DNA. Through the use of isothermal heatburst microcalorimetry, the assembly of the H2A–H2B dimer and (H3–H4)₂ tetramer into an H2A–H2B–(H3–H4)₂ hexamer and subsequently into an (H2A–H2B–H3–H4)₂ octamer was found to have large and unequal enthalpies at neutrality in high salt ($\Delta H_1 > \Delta H_2$). Cooperativity in the assembly process was observed, with the equilibrium constant of the second step being 4 times greater than that of the first step. The large heats suggest hydrogen bonding as the predominant interaction between the subunits.

Since no other studies have been performed on the protein constituents of the nucleosome core, we have initiated a systematic study to examine the energetics of the core histone octamer as well as octamer–DNA interactions as they pertain to nucleosome stability. As a first step in these studies, we present here our results on the simplest thermodynamic entity of this system, i.e., the H2A–H2B dimer subunit. This subunit has been studied over the ionic strength and pH ranges where the interaction of the dimer with the (H3–H4)₂ tetramer subunit was found earlier to be particularly sensitive (Eickbush & Moudrianakis, 1978). The calorimetric and spectroscopic experiments provide a thermodynamic basis for explaining previous biochemical and structural observations regarding the stability of the H2A–H2B dimer and emphasize the significance of the H2A–H2B interface in the stability of the folded state of the polypeptides of this subunit.

MATERIALS AND METHODS

Isolation of Histones. Chicken erythrocyte histones were isolated by a modification of the salt extraction procedure previously used in this laboratory (Eickbush & Moudrianakis, 1978). The H2A–H2B dimer was efficiently separated from the (H3–H4)₂ tetramer on a CM-cellulose (Whatman CM-52) column equilibrated with 0.1 M potassium phosphate, 1 mM EDTA, and 0.5 M urea, pH 6.7, and eluted using a 0.1–0.6 M KCl stepwise gradient. All isolation steps were performed at 4 °C, with repeated additions of PMSF.

Sample Preparation. Histone dimer samples were dialyzed into the desired pH and NaCl-containing buffers overnight to assure dialysis equilibrium. The DSC experiments in higher ionic strength were performed in 0.15–4.0

M NaCl, 1 mM EDTA, and 10 mM sodium phosphate, pH 7.5. Samples for the DSC lower ionic strength series at neutrality were prepared in solutions containing 0.0–140 mM NaCl, 1 mM EDTA, and 10 mM imidazole, pH 7.5. For the DSC pH series experiments, samples were dialyzed into solutions containing 50 mM NaCl and ranging in pH from 3.5 to 11.5. The buffers used were 10 mM glycylglycine for pH 3.5–4.5 and 8.5, 10 mM imidazole for pH 5.5–7.5, and 10 mM glycine for pH 9.5–11.5. Samples for the CD ionic strength experiments were prepared in 0.05–1.0 M NaCl solutions containing 0.1 mM EDTA, 10 mM HEPES, pH 7.5. The CD pH series experiments were performed in solutions containing 100 mM NaCl and ranging in pH from 2.5 to 11.5. The buffers used were 10 mM glycine for pH 2.5–4.0, 10 mM MES for pH 4.5–5.5, 10 mM HEPES for pH 6.5–7.5, 10 mM bicine for pH 8.5–9.5, and 7.5 mM CAPS for pH 10.5–11.5. Protein concentrations used were 2 mg/mL for the DSC experiments and 0.3 mg/mL for the CD experiments. The concentrations were determined spectrophotometrically immediately prior to performing scans as previously described (Godfrey et al., 1990). Protein purity was assayed on 20% acrylamide–0.1% NaDodSO₄/polyacrylamide gels (Laemmli, 1970). Proteins were visualized by bathing the gels in 40% ethanol, 5% acetic acid, and 0.1% Coomassie Brilliant Blue R_i. Gels were subsequently destained with 20% ethanol, 5% acetic acid. Gels of protein preparations used in this study revealed only the appropriate core histones with no detectable breakdown products.

Differential Scanning Calorimetry. Calorimetric scans at higher ionic strength were performed using a Microcal (Northampton, MA) MC-2 differential scanning calorimeter. A scan rate of 30 °C/h was used in these experiments. Experiments at lower ionic strength at neutrality and in the pH series were scanned at a rate of 60 °C/h in a DASM-4M microcalorimeter under 60 kg/cm N₂ pressure.

In all DSC experiments, the calorimetric unit was interfaced to an IBM PC microcomputer using analog-digital converter (Data Translation DT-2801) for automatic data collection and analysis.

To test for the ability of the H2A–H2B dimer to renature, all samples were cooled at the end of the first scan, allowed to reequilibrate to the starting temperature, and then scanned again. The percent renaturation is expressed as the ΔH_{cal} of the second scan divided by that of the first. The excess heat capacity function was analyzed after normalization and base-line subtraction using programs developed at the Biocalorimetry Center.

Circular Dichroism. All CD measurements were performed in a Jasco J-710 spectropolarimeter interfaced to an IBM PC microcomputer for automatic data collection and analysis. Temperature scans were performed by scanning continuously from 6 to 80 °C in a 1 mm rectangular quartz cell (Hellma Scientific).

Temperature was controlled using a Haake PG20 temperature programmer interfaced to a Haake F3 circulating water bath, with a rate of increase in temperature of 60 °C/h. Temperature was monitored using a Microtherm 1006 thermometer and an S/N 117C temperature probe just outside of the sample cell. Data were collected using the time scan mode within the J-710 software package. The ellipticity at 222 nm was recorded every 20 s with a response time of 1 s and a bandwidth of 1 nm. The ellipticity and the temperature were manually recorded at discrete intervals of

5 °C, and intermediate temperatures were interpolated for every intervening ellipticity reading to yield a complete description of Θ_{222} vs temperature. Ellipticity readings were normalized to the fraction unfolded using the equation:

$$P_u = (\Theta - \Theta_N) / (\Theta_D - \Theta_N)$$

where Θ_D and Θ_N represent the ellipticity values for the fully unfolded and fully folded state at each temperature, as calculated from the slopes of the base lines preceding and following the transition region.

RESULTS AND DISCUSSION

Ionic Strength Dependence of the Melting of the H2A–H2B Dimer. The histone H2A–H2B dimer was analyzed by differential scanning calorimetry and circular dichroism spectroscopy over the ionic strength range where its interaction with the histone (H3–H4)₂ tetramer is particularly sensitive (Eickbush & Moudrianakis, 1978). A family of high-sensitivity calorimetric scans of the histone dimer was obtained at pH 7.5 and at salt concentrations ranging from 0.05 to 4.0 M NaCl (Figure 1a). As shown in Figure 1b, the transition temperature increases from 52.4 °C at 0.05 M NaCl to 80.4 °C at 4.0 M NaCl. The transition was better than 75% reversible up to a salt concentration of 0.3 M. Above that salt concentration, the transition became progressively irreversible. It appears that the increase in ionic strength promotes self-aggregation of the histone dimer. For this reason, a complete thermodynamic analysis was performed only for the data obtained at low ionic strength conditions. The basis for the ionic strength-dependent aggregation is currently under investigation. Since the histone dimer exhibited nonideal behavior under conditions that promote its assembly with the (H3–H4)₂ tetramer, calorimetric scans were instead performed in low ionic strength conditions (0–140 mM NaCl), where almost complete reversibility is observed (Table 1). At 140 mM NaCl, the transition of the histone dimer is characterized by the presence of a single peak located at about 52 °C, an enthalpy change of about 42 kcal/mol of 14 kDa monomer unit, and a heat capacity difference between the unfolded and the native states (ΔC_p) of about 1.5 kcal/(K·mol) of 14 kDa monomer unit.

As illustrated in Figure 1a, the transition temperature and the enthalpy change decrease as the ionic strength decreases (see also Table 1). The straight line relationship between ΔH_{cal} and T_m ($r = 0.98$) yields a ΔC_p of 1.3 kcal/(K·mol) of 14 kDa monomer unit, or 0.09 cal/(g·K), which is of the same order previously reported for other proteins (Privalov & Khechinashvili, 1974) and close to the one measured directly from individual scans. The unfolding transition is coupled to the dissociation of the two subunits of the H2A–H2B dimer, as indicated by the concentration dependence of the transition temperature. This effect is also reflected by the asymmetry of the heat capacity function, which in all cases is skewed toward the low-temperature side of the transition, as expected for a transition coupled to dissociation (Freire, 1989). In all the calorimetric experiments presented in Figure 1a, the transitions were highly reversible (77–94%), as demonstrated by the recovery of the original signal in a repeated scan of the same sample (Table 1).

A similar family of CD temperature scans at constant wavelength was performed on samples dialyzed against

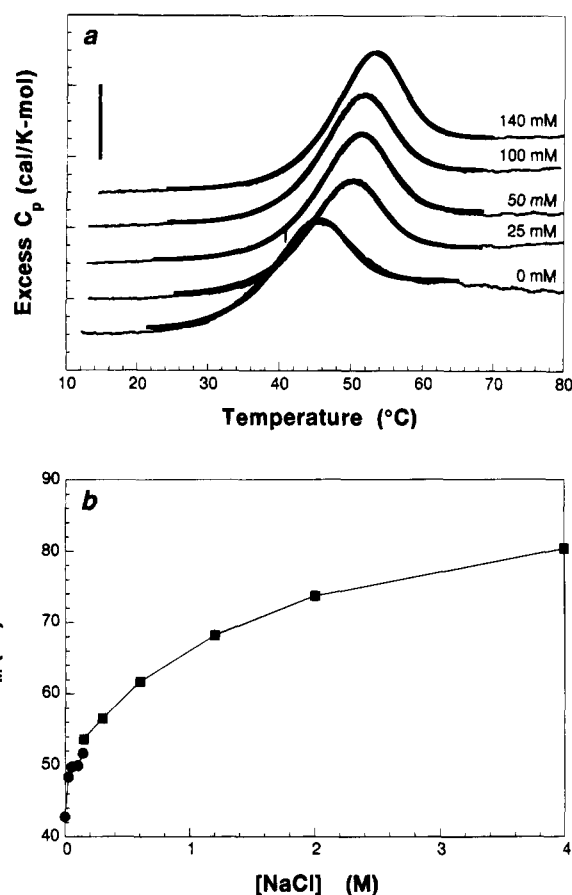


FIGURE 1: (a) Excess heat capacity of the H2A–H2B dimer as a function of ionic strength. The NaCl concentrations are, from bottom to top, 0, 25, 50, 100, and 140 mM. Experiments were performed in 1 mM EDTA, 10 mM imidazole, pH 7.5. The protein concentration was kept constant at 130 μ M 14 kDa monomer unit. Experimental data are represented by thin solid lines. Theoretical curves generated with the parameters shown in Table 1 are represented by thick solid lines. For clarity of presentation, the data sets have been offset by 1 kcal/(K·mol) below the 140 mM NaCl data set. Vertical bar equals 2 kcal/(K·mol). (b) Melting temperatures of the H2A–H2B dimer as a function of ionic strength using differential scanning calorimetry. Experiments were performed in 0.0–4.0 M NaCl, 1 mM EDTA, and 10 mM imidazole, pH 7.5. T_m represents the temperature corresponding to $C_{p,max}$.

0.05–1.0 M NaCl, as shown in Figure 2a. The stability of the histone dimer increases as a function of ionic strength. The transition temperature increases from 43.2 °C at 0.05 M NaCl to 67.3 °C at 1.0 M NaCl, in a way very similar to the one observed in the DSC experiments.

pH Dependence of the Melting of the H2A–H2B Dimer. The thermal unfolding behavior of the H2A–H2B dimer at low ionic strength was examined in solutions ranging from pH 2.5 to 11.5 by differential scanning calorimetry and circular dichroism spectroscopy. The thermal denaturation profiles from the DSC scans are shown in Figure 3a,b. The T_m of the H2A–H2B dimer remains essentially the same between pH 6.5 and pH 9.5 (about 47 °C), whereas it decreases substantially below pH 5.0 and above pH 10.0 (Figure 3c). The histone dimer exhibits maximum reversibility between pH 4.5 and 8.5 (85–100%), whereas its ability to renature upon cooling is greatly reduced above pH 9.0 (Table 2). In the region of pH where the system is reversible, the calorimetric enthalpy change follows a similar pattern to the one exhibited by T_m , in that ΔH_{cal} remains

Table 1: Fitted Thermodynamic Parameters Associated with the Unfolding of the H2A–H2B Dimer as a Function of Ionic Strength^a

	[NaCl] (mM)	T_m (°C)	T° (°C)	$\Delta H(T^\circ)$ (kcal mol ⁻¹)	$\Delta S(T^\circ)$ [cal (K·mol) ⁻¹]	ΔC_p^c [kcal (K·mol) ⁻¹]	SSR ^d	% rev ^e
DSC	0	42.8	65.8	53.4	158	1.0	80	86
	25	48.4	66.4	62.0	183	1.4	55	92
	50	49.8	67.5	63.2	186	1.3	46	94
	100	50.0	68.1	63.3	185	1.4	63	85
	140	51.7	68.6	67.0	196	1.5	35	77
CD	50	43.6	64.1	65.2	193		0.02	
	100	48.5	68.6	68.6	201		0.02	
	200	53.7	74.0	72.5	209		0.02	
	400	58.6	77.5	78.3	224		0.02	
	1000	67.4	84.5	86.7	243		0.03	

^a All thermodynamic parameters are expressed on a per 14 kDa monomer unit basis. ^b T° is the temperature at which the intrinsic free energy ΔG° is equal to zero and should be independent of concentration. ^c ΔC_p was calculated from the observed difference in heat capacity between the unfolded and the native state. ^d SSR is the sum of the squared residuals of the fit. ^e % rev is the percent reversibility of the DSC scans.

Table 2: Fitted Thermodynamic Parameters Associated with the Unfolding of the H2A–H2B Dimer as a Function of pH^a

	pH	T_m (°C)	T° (°C)	$\Delta H(T^\circ)$ (kcal·mol ⁻¹)	$\Delta S(T^\circ)$ [cal (K·mol) ⁻¹]	ΔC_p^c [kcal (K·mol) ⁻¹]	SSR ^d	% rev ^e
DSC	4.5	36.4						85
	5.5	43.6	64.2	52.3	155	0.9	116	100
	6.5	47.4	63.5	61.1	182	1.4	40	96
	7.5	47.2	63.8	62.1	184	1.5	31	99
	8.5	49.4	65.5	62.9	186	1.4	31	90
	9.5	48.2	66.1	61.1	180	1.3	222	60
	10.5	39.6						8
	11.5	37.5						0
CD	4.0	32.0						
	4.5	34.3						
	5.5	42.4	65.1	64.1	190		0.03	
	6.5	45.0	66.5	66.6	197		0.02	
	7.5	46.1	67.3	67.5	198		0.02	
	8.5	47.3	68.1	68.5	201		0.03	
	9.5	46.2	65.7	68.0	201		0.04	
	10.5	37.6						
	11.5	32.0						

^a All thermodynamic parameters are expressed on a per 14 kDa monomer unit basis. ^b T° is the temperature at which the intrinsic free energy ΔG° is equal to zero and should be independent of concentration. ^c ΔC_p was calculated from the observed difference in heat capacity between the unfolded and the native state. ^d SSR is the sum of the squared residuals of the fit. ^e % rev is the percent reversibility of the DSC scans.

essentially constant from pH 6.5 to pH 9.5 (at about 38 kcal/mol of 14 kDa monomer unit).

The magnitude of the calorimetric enthalpy change decreases below pH 6.0; above pH 10.0, it initially increases (at pH 10.5) and then decreases while the T_m decreases. This pH-dependent increase in ΔH_{cal} above pH 10.0 is accompanied by a significant sharpening of the calorimetric peak which cannot be accounted for by the high ΔH_{cal} alone and is indicative of higher order interactions. It is likely that self-aggregation of the histone dimer takes place above pH 10.0; such aggregation may be promoted by the neutralization of the protein positive charges as the pH approaches the pK_a of the H2A–H2B dimer. A summary of the T_m , ΔH_{cal} , and reversibility values as a function of pH is provided in Table 2. The straight line relationship between ΔH_{cal} and T_m ($r = 0.98$), from pH 5.5 to pH 9.5, provides a ΔC_p value equal to 1.1 kcal/(K·mol) of 14 kDa monomer unit, or 0.08 cal/(g·K), which is comparable to the one determined from the ionic strength DSC series already described.

A very similar family of thermal denaturation profiles below and above pH 7.5 was obtained by CD temperature scans, providing results that essentially duplicate the calorimetric data. The CD melting curves are presented in Figure 4a,b, and the dependence of T_m on pH, as determined spectroscopically, is shown in Figure 4c. From both the calorimetric and the spectroscopic experiments, it seems that

the histone H2A–H2B dimer is almost completely unfolded below pH 4.0, within the whole temperature range examined. This is indicated by the absence of any transition peak for the calorimetric scan at pH 3.5 and by the fact that the fraction unfolded equals unity at all temperatures for the CD scans at pH 3.5 and 2.5 (Figures 3a and 4a).

Circular dichroism experiments indicate that the α -helical content of the H2A–H2B dimer as a function of pH follows a pattern that parallels and is consistent with the pH dependence of the T_m of the dimer unfolding transition. The α -helical content is maximum and essentially constant between pH 5.5 and 10.5, whereas it decreases below pH 5.0 and above pH 11.0. An even more radical decrease in the α -helical content of the H2A–H2B dimer takes place below pH 4.0 (Figure 5). It should be noticed that a well-defined single isodichroic point is observed at 205 nm, which is consistent with the behavior of a system with only two, optically distinguishable conformations.

Protein Concentration Dependence of H2A–H2B Dimer Melting. The thermal unfolding behavior of the H2A–H2B dimer as a function of protein concentration was examined in solutions of low ionic strength. The concentration of the protein in the reaction was varied between 2.0 and 110 μ M, this concentration expressed on the basis of the molecular mass of the monomer polypeptide, i.e., 14 kDa. The thermal denaturation profiles were monitored by CD spectroscopy,

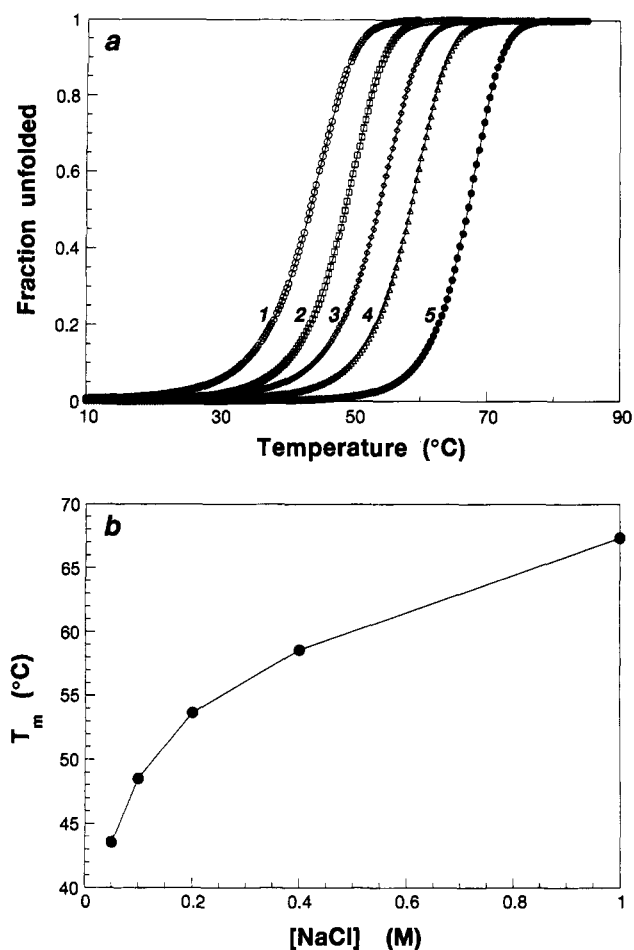


FIGURE 2: (a) Fraction of H2A–H2B dimer unfolded at increasing ionic strength as a function of temperature. The NaCl concentrations are 50 mM (open circles), 100 mM (squares), 200 mM (diamonds), 400 mM (triangles), and 1 M (filled circles). Experiments were performed in 0.1 mM EDTA, 10 mM HEPES, pH 7.5. The protein concentration was kept constant at 22 μ M 14 kDa monomer unit. Fraction unfolded was monitored by the ellipticity at 222 nm using CD spectroscopy. Experimental data are represented by symbols. Theoretical curves generated with the parameters shown in Table 1 are represented by solid lines. (b) Melting temperatures of the H2A–H2B dimer as a function of ionic strength using CD spectroscopy. T_m represents the temperature at which the fraction unfolded is equal to 0.5.

and the results are shown in Figure 6a. It is obvious that the transition shifts to higher temperatures as the concentration of the protein is increased. The T_m of the thermal unfolding (shown in Figure 6b) increases from 43.0 to 51.3 °C as the protein concentration is increased from 2.0 to 110 μ M, as expected for an associating system where the order of the monomer subunits increases upon association. A summary of the T_m , T° , and $\Delta H(T^\circ)$ values from the protein concentration series of CD and the corresponding DSC experiments is shown in Table 3.

Statistical Thermodynamic Analysis. Since the folding/unfolding transition of the histone H2A–H2B dimer is characterized by the presence of a single peak, we decided to investigate if this transition actually involves only two states (folded dimer and unfolded monomers) or includes the presence of a significant population of intermediates (folded monomers). For this purpose, the calorimetric data from the low ionic strength conditions were analyzed in terms of the complete statistical thermodynamic equations for the three-state system in a manner analogous to that described

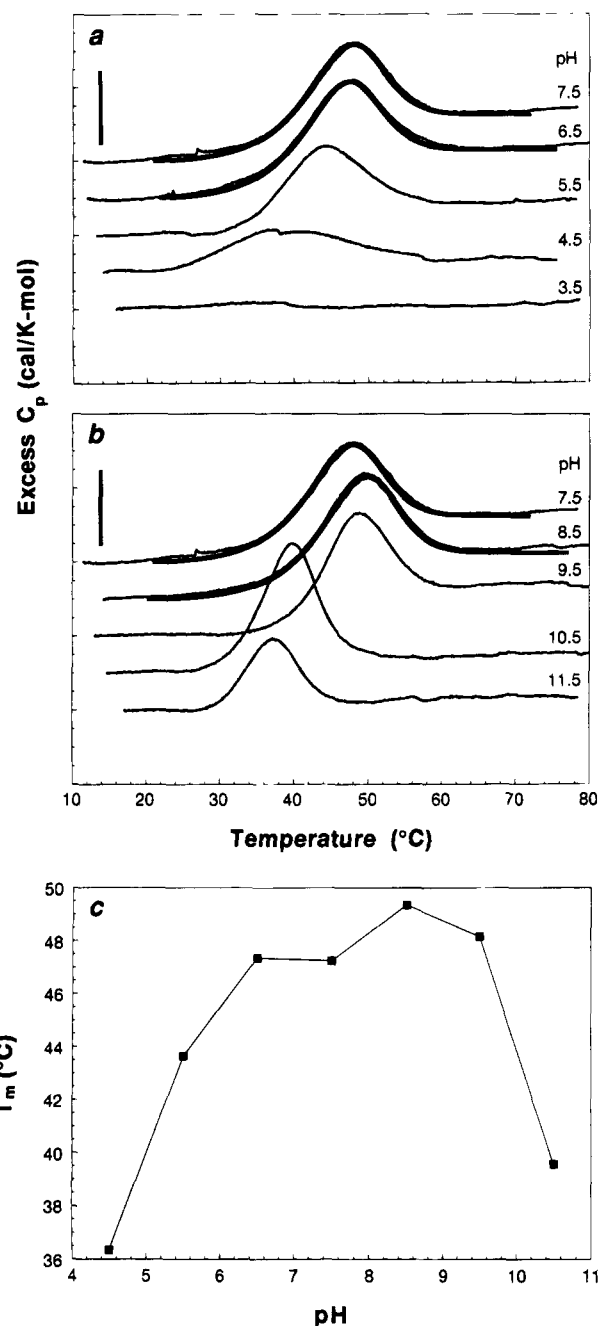


FIGURE 3: Excess heat capacity of the H2A–H2B dimer as a function of pH. (a) pH values are, from top to bottom, 7.5, 6.5, 5.5, 4.5, and 3.5. (b) pH values are, from top to bottom, 7.5, 8.5, 9.5, 10.5, and 11.5. Experiments were performed in 50 mM NaCl, 10 mM appropriate pH buffer (see Materials and Methods). The protein concentration was kept constant at 144 μ M 14 kDa monomer unit. Experimental data are represented by thin solid lines. Theoretical data are represented by thick solid lines. For clarity of presentation, the data sets have been offset by 1 kcal/(K·mol) below the pH 7.5 data set. Vertical bar equals 2 kcal/(K·mol). (c) Melting temperatures of the H2A–H2B dimer as a function of pH using differential scanning calorimetry. T_m represents the temperature corresponding to $C_{p,max}$.

for the thermodynamic characterization of the structural stability of the coiled-coil region of the bZIP transcription factor GCN4 (Thompson et al., 1993). The experimental excess heat capacity data (ΔC_p vs temperature) were analyzed in terms of the three-state formalism using a nonlinear least-squares procedure as described elsewhere (Ramsay & Freire, 1990). In all cases studied in the low ionic strength

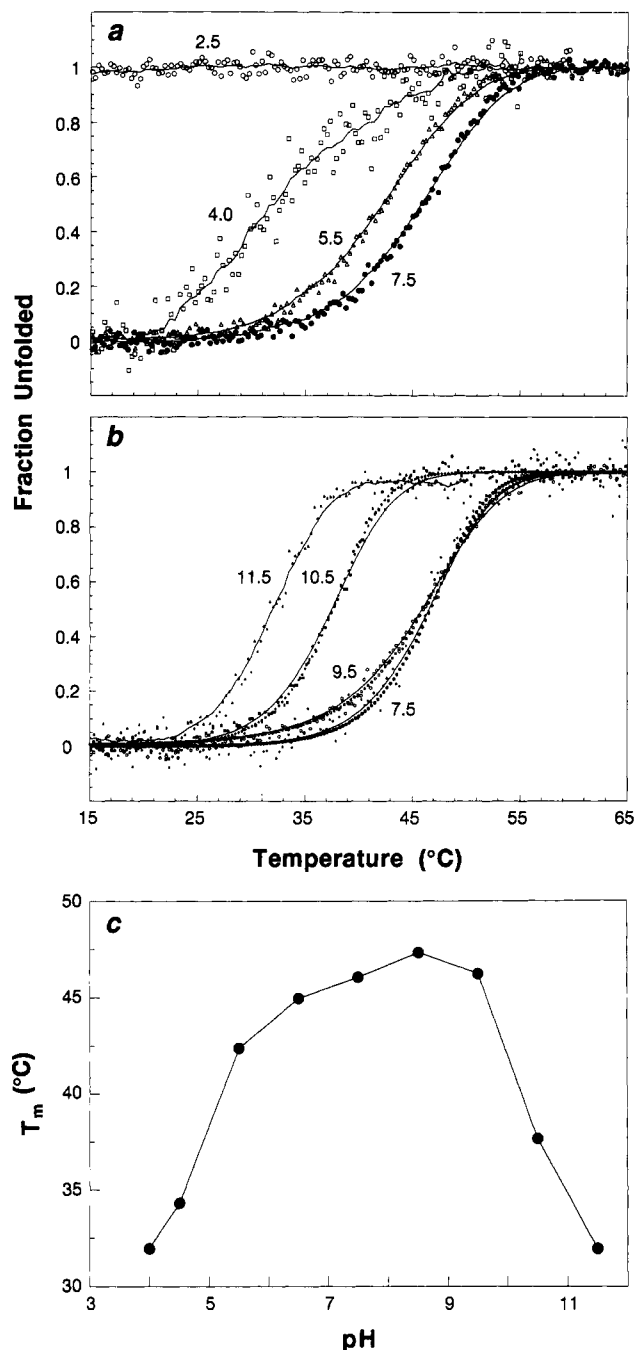


FIGURE 4: Fraction of H2A–H2B dimer unfolded at different pH values as a function of temperature. (a) pH values are 7.5 (filled circles), 5.5 (triangles), 4.0 (squares), and 2.5 (open circles). (b) pH values are 7.5 (filled circles), 9.5 (open squares), 10.5 (filled squares), and 11.5 (filled triangles). Experiments were performed in 100 mM NaCl, 10 mM appropriate pH buffer. The protein concentration was kept constant at 20 μ M 14 kDa monomer unit. The fraction unfolded was monitored by the ellipticity at 222 nm using CD spectroscopy. Experimental data are represented by symbols. Theoretical curves generated with the parameters shown in Table 2 are represented by solid lines. (c) Melting temperatures of the H2A–H2B dimer as a function of pH using CD spectroscopy. T_m represents the temperature at which the fraction unfolded is equal to 0.5.

environment, it was found that intermediate conformations were nondetectable and did not contribute, in any measurable way, to the obtained calorimetric signal. Therefore, the thermal unfolding transition of the histone H2A–H2B dimer was well represented by a two-state mechanism in which the only states significantly populated at all temperatures

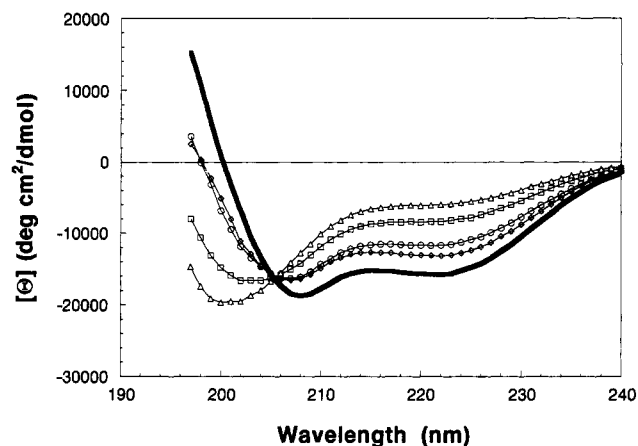


FIGURE 5: Far-UV CD spectra of the H2A–H2B dimer at different pH values. Experiments were performed in 100 mM NaCl, 10 mM appropriate pH buffer. The protein concentration was kept constant at 20 μ M 14 kDa monomer unit. The pH values are 5.5–10.5 (thick solid line), 11.5 (diamonds), 4.5 (open circles), 4.0 (squares), and 2.5 (triangles).

were native dimer and unfolded monomers. In such case, at any temperature the population of unfolded monomers is given by the equation (Thomson et al., 1993):

$$P_U = P_{H2A} + P_{H2B} = K[(K^2 + 4)^{1/2} - K]/2$$

where

$$K = \exp(-\Delta G^\circ/RT)/(2[P_T])^{1/2}$$

The equilibrium constant, K , is a function of the protein concentration, $[P_T]$, as well as the intrinsic free energy of stabilization, ΔG° . For convenience, all thermodynamic quantities are expressed on a per mole of single polypeptide chain basis. The intrinsic Gibbs energy is given by the standard equation:

$$\Delta G^\circ = \Delta H^\circ(T^\circ) + \Delta C_p(T - T^\circ) - T[\Delta S^\circ(T^\circ) + \Delta C_p \ln(T/T^\circ)]$$

where by definition T° is the temperature at which ΔG° is equal to zero. This temperature is independent of concentration and should not be confused with the transition temperature which is concentration-dependent. Contrary to the case of a monomeric two-state transition, in this case the transition temperature T_m is not equal to the temperature at which $\Delta G^\circ = 0$. Also, because a transition involving dissociation is asymmetrical, the temperature of a maximum in the heat capacity function does not coincide with the temperature at which half of the molecules have undergone the transition. In this paper, the reported T_m values correspond to the temperature of the maximum in the heat capacity function.

The thick solid lines in Figure 1a correspond to the theoretical curves with the best fit parameters to the experimental data analyzed by the nonlinear squares procedure mentioned above.

The ionic strength series of CD experiments were also analyzed in terms of the above formalism. The experimental data and the corresponding theoretical curves are presented in Figure 2a. In these experiments, which are performed at substantially lower protein concentration, data obtained under comparatively high ionic strength conditions (<1 M NaCl) could still be fitted to the two-state model described above. On the basis of this observation, the histone dimer self-

Table 3: Fitted Thermodynamic Parameters Associated with the Unfolding of the H2A–H2B Dimer as a Function of Protein Concentration^a

	14 kDa monomer unit concn (μM)	T_m ($^{\circ}\text{C}$)	T° ^b ($^{\circ}\text{C}$)	$\Delta H(T^{\circ})$ (kcal mol ⁻¹)	$\Delta S(T^{\circ})$ [cal (K·mol) ⁻¹]	ΔC_p ^c [kcal (K·mol) ⁻¹]	SSR ^d
CD	2.0	43.0	69.2	58.7	172		0.03
	5.0	45.6	68.5	60.7	178		0.02
	21.6	48.2	68.3	62.5	183		0.02
	43.3	49.5	68.4	63.0	184		
	98.6	50.1	67.2	63.5	187		0.01
DSC	110.0	51.3	66.9	66.6	196	1.5	61

^a All thermodynamic parameters are expressed on a per 14 kDa monomer unit basis. ^b T° is the temperature at which the intrinsic free energy ΔG° is equal to zero and should be independent of concentration. ^c ΔC_p was calculated from the observed difference in heat capacity between the unfolded and the native state. ^d SSR is the sum of the squared residuals of the fit.

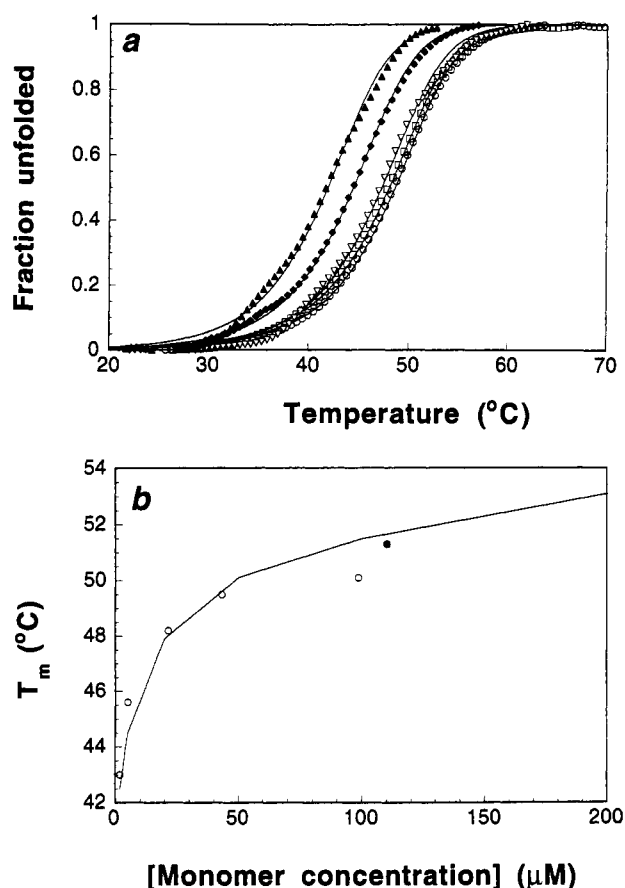


FIGURE 6: (a) Fraction of H2A–H2B dimer unfolded at increasing protein concentration as a function of temperature. The 14 kDa monomer unit concentrations are 2.0 μM (filled triangles), 5.0 μM (filled diamonds), 21.6 μM (inverted triangles), 43.3 μM (squares), and 98.6 μM (open circles). Experiments were performed in 50 mM NaCl, 0.1 mM EDTA, and 10 mM HEPES, pH 7.5. The fraction unfolded was monitored by the ellipticity at 222 nm using CD spectroscopy. Experimental data are represented by symbols. Theoretical curves generated with the parameters shown in Table 3 are represented by solid lines. (b) Melting temperatures of the H2A–H2B dimer as a function of monomer unit protein concentration. The open circles represent CD data; the filled circle represents DSC data. The solid line is a best-fit logarithmic curve through theoretical transition temperatures, as calculated according to the model that predicts the coupling between unfolding and dissociation of the H2A–H2B dimer.

aggregation appears to be both ionic strength- and protein concentration-dependent.

The fitted thermodynamic parameters associated with the unfolding of the histone H2A–H2B dimer, as a function of ionic strength, have been summarized in Table 1 for both the DSC and CD experimental series. It is obvious that

similar parameter values were obtained from the analysis of the calorimetric and spectroscopic data. For example, at 100 mM NaCl at T° , the enthalpy change measured calorimetrically is 63.3 kcal/mol of 14 kDa monomer unit compared to the value of 68.6 kcal/mol of 14 kDa monomer unit measured spectroscopically. The entropy change determined by DSC is 185 cal/(K·mol) of 14 kDa monomer unit, and the one determined by CD is 201 cal/(K·mol) of 14 kDa monomer unit. The corresponding T° value determined by DSC is 68.1 $^{\circ}\text{C}$, while that determined by CD is equal to 68.6 $^{\circ}\text{C}$.

The two-state model that so well represented the unfolding transitions of the histone H2A–H2B dimer in the low ionic strength series at neutrality was also used for fitting the calorimetric and spectroscopic data as a function of pH. In this case, the single-cooperative-unit formalism described accurately the melting profile of the H2A–H2B dimer between pH 6.5 and 8.5. As it was observed for the low ionic strength series at neutrality, likewise, between pH 6.5 and 8.5 the histone H2A–H2B dimer undergoes a two-state folding/unfolding transition with only two states populated at all temperatures, those of the native dimer and the unfolded monomers. Outside this relatively narrow pH range, the application of the simple two-state model described above is inappropriate, as shown in Table 2 by the abrupt increase in the sum of the squared residuals of the fit for the DSC scans at pH 5.5 and 9.5. Table 2 also includes the fitted thermodynamic parameters associated with the unfolding of the histone dimer between pH 6.5 and 8.5 for both the DSC and CD experimental series. The values of the parameters obtained from the analysis of the calorimetric and spectroscopic pH experiments of the pH 6.5–8.5 set were comparable to those obtained from the low ionic strength data at neutrality, described in the first part of this paper.

The model developed above and the resulting parameters accurately describe the protein concentration dependence of the transition temperature, as shown in Figure 6b in which the transition temperatures from the CD data series (and one DSC experiment) have been plotted as a function of monomer protein concentration. Thus, the validity of the model which predicts the coupling between unfolding and dissociation of the chains of the histone dimer was checked both by the goodness of the fit of the DSC and CD data and by the protein concentration dependence of the T_m .

The analogous calorimetric experiments from the low ionic strength series at neutrality and from the pH series should result in identical thermodynamic parameters. In our case, the ionic strength series experiment at 50 mM NaCl gave a peak with $T^{\circ} = 67.5$ $^{\circ}\text{C}$ and $\Delta H_{\text{cal}}(T^{\circ}) = 63.2$ kcal/mol of 14 kDa monomer unit, whereas the corresponding experiment

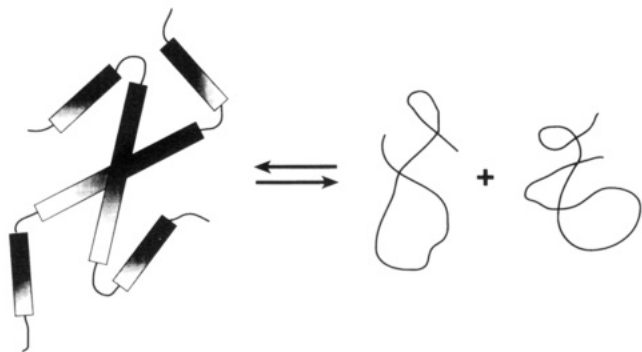


FIGURE 7: Schematic representation of the two-state mechanism that accounts for the thermal unfolding of the H2A–H2B dimer. No folded monomer intermediates are present at any stage of this equilibrium under the experimental conditions of this study.

from the pH series gave a peak with $T^\circ = 63.8^\circ\text{C}$ and $\Delta H_{\text{cal}}(T^\circ) = 62.1$ kcal/mol of 14 kDa monomer unit. The difference of 3.7°C in T° between the two experiments most likely represents the effect of 1 mM EDTA on the thermal stability of the histone H2A–H2B dimer. As described under Materials and Methods, EDTA was included in the solutions of the ionic strength series, whereas no EDTA was added to the buffers of the pH experiments. A systematic increase in EDTA concentration (unpublished experiments) suggests that a simple ionic strength effect brought about by the addition of EDTA in the buffer does not appear to be sufficient to account for these results. This phenomenon is under investigation.

The model described above and the resulting parameters clearly show that at neutral pH and low ionic strength the histone H2A–H2B dimer undergoes a temperature unfolding transition as a single cooperative unit, without any measurable intermediates of stably folded H2A and H2B monomers. This implies that at the point where thermal denaturation occurs, cooperative interactions within the dimer are the most important contributors to the stability of the system. That is, as soon as conditions that eliminate these interactions have been reached, the individual chains are unable to exhibit any degree of folding; i.e., the isolated monomers are intrinsically unstable at those conditions. The relative contributions of the two chains to the overall stability of the system cannot be estimated from these experiments, and they do not necessarily have to be equal. However, their association is responsible for the manifested thermodynamic stability of the dimer. The coupled dissociation and unfolding of the H2A–H2B dimer can be represented by the general scheme $AB \rightarrow 2U$ (see also Figure 7). The high cooperativity of the system is consistent with the fact that the functional subunit of the histone core octamer is the H2A–H2B dimer itself and not the individual H2A and H2B monomers, which cannot be actually detected as independent entities in solution.

As it became clear early on in chromatin research, single histone chains are not observed as stably folded polypeptides in biologically-relevant solutions. Instead, they are found as individual polypeptides and in the random coil configuration only when dissolved in pure water or acids. Increasing salt concentration has the effect of inducing and promoting secondary structure in histones (Bradbury et al., 1965; Isenberg, 1974). However, in salt solutions, the histones inevitably undergo homotypic or heterotypic associations, depending on the classes of histones present. This is

particularly true for the individual histones H3 and H4, which tend to form large, aggregated structures even at low ionic strength conditions (Shih & Bonner, 1970; Olins & Olins, 1971; Ansevin & Brown, 1971; Shih & Fasman, 1971). Histones H2A and H2B also exhibit self-association, given sufficiently high histone and salt concentrations (Edwards & Shooter, 1969; Diggle & Peacocke, 1971). The potential significance of the specific associations of histones was realized by Rubin and Moudrianakis (1972), who proposed that histone/histone interactions “may involve associations of specific histone classes and result in structures that depend on the juxtaposition of certain classes of histones” (Rubin & Moudrianakis, 1972). Subsequent work (D’Anna & Isenberg, 1974; Rubin & Moudrianakis, 1975; Roark et al., 1976) established currently accepted histone patterns for histone–histone associations. Finally, it has been documented that the H2A–H2B dimer and the $(\text{H3–H4})_2$ tetramer are the soluble entities under which histones are found in most biologically relevant conditions, including those leading to the reversible self-assembly of the core histone octamer (Eickbush & Moudrianakis, 1978). The importance of the H2A–H2B and H3–H4 pairwise associations is further supported by the fact that these interaction patterns have been extremely well conserved through evolution (yeast: Mardian & Isenberg, 1978; *Tetrahymena*: Glover & Gorovsky, 1978; pea: Spiker & Isenberg, 1977). The high cooperativity in the unfolding of the H2A–H2B dimer presented in this paper is in perfect agreement with all the data described above and actually provides a physical basis for their explanation: histone/histone interactions are absolutely critical for the structural stabilization of the individual monomers.

Finally, from a protein folding point of view, the fact that the unfolding transition of the H2A–H2B heterodimer is well-described by a two-state process is of particular interest. Since states of individually-folded polypeptides cannot be detected, one is led to conclude that the energy of stabilization of the dimer derives primarily from cooperative interactions along the contact interfaces between H2A and H2B. The same explanation appears to account for the temperature unfolding of the dimerization domain (leucine zipper) of the bZIP transcription factor GCN4 (Thompson et al., 1993), which is a homodimer of two small polypeptides. In contrast, the H2A and H2B polypeptides have molecular weights of ca. 13 500 and have different primary structures (only 4–6% identity). However, although their primary sequences are quite different, the H2A and H2B proteins share a common way of secondary and tertiary folding, the *histone fold* (Arents et al., 1991), which may be responsible for their thermodynamically indistinguishable melting behavior. Within this fold, the individual polypeptides are folded in a similar manner, most noticeably in the central portion of each chain. The common motif consists of a long central helix, flanked on either side by a loop/strand segment and a shorter helix. The pairwise association follows a characteristic “handshake” motif; that is, rather than assembling like the globular domains of the α and β chains of the hemoglobin dimer, which have small local contacts, the H2A and H2B polypeptides, by clasping each other, develop an extensive molecular contact interface within the H2A–H2B dimer. The thermodynamic data presented here are in accord with the expectations derived from that structure, i.e., that the stability of that dimer is dependent on the intermolecular associations between the H2A and H2B intradimer

interface. Furthermore, the present data demonstrate that once these interactions are eliminated the individual chains cannot retain their characteristic secondary structure under any experimental conditions tested thus far.

CONCLUSIONS

The thermal stability of the core histone H2A–H2B dimer has been studied as a function of ionic strength and pH. In low ionic strength conditions and pH values between 6.5 and 8.5, the folding/unfolding transition of the H2A–H2B dimer is highly cooperative and is characterized by the absence of folded monomers; the only two states that can account for essentially the entire population of molecules are the native dimer and the unfolded monomers. The unfolding transition temperature of the H2A–H2B dimer increases as a function of ionic strength. Elevated salt concentrations promote the self-aggregation of the histone dimer, and, therefore, the complete thermodynamic analysis was performed only on data obtained in low ionic strength conditions. The H2A–H2B dimer appears to be a stable complex between pH 5.5 and 10.5. Its stability is rapidly decreased outside this pH range. Complete unfolding occurs below pH 4.0.

REFERENCES

- Ansevin, A. T., & Brown, B. W. (1971) *Biochemistry* 10, 1139.
- Arents, G., Burlingame, R. W., Wang, B.-C., Love, W. E., & Moudrianakis, E. N. (1991) *Proc. Natl. Acad. Sci. U.S.A.* 88, 10148.
- Benedict, R. C., Moudrianakis, E. N., & Ackers, G. K. (1984) *Biochemistry* 23, 1214.
- Bina, M., Sturtevant, J. M., & Stein, A. (1980) *Proc. Natl. Acad. Sci. U.S.A.* 77, 4044.
- Bradbury, E. M., Crane-Robinson, C., Phillips, D. M. P., Johns, E. W., & Murray, K. (1965) *Nature (London)* 205, 1315.
- D'Anna, J. A., & Isenberg, I. (1973) *Biochemistry* 12, 1035.
- D'Anna, J. A., & Isenberg, I. (1974) *Biochemistry* 13, 4992.
- Diggle, J. H., Mc Vittie, J. D., & Peacocke, A. R. (1975) *Eur. J. Biochem.* 56, 173.
- Edwards, P. A., & Shooter, K. V. (1969) *Biochem. J.* 114, 227.
- Eickbush, T. H., & Moudrianakis, E. N. (1978) *Biochemistry* 17, 4955.
- Freire, E. (1989) *Comments Mol. Cell. Biophys.* 6, 123.
- Glover, C. V. C., & Gorovsky, M. A. (1978) *Biochemistry* 17, 5705.
- Kornberg, R. D. (1974) *Science (Washington, D.C.)* 184, 868.
- Laemmli, U. K. (1970) *Nature (London)* 227, 680.
- Mardian, J. K. W., & Isenberg, I. (1978) *Biochemistry* 17, 3825.
- Olins, D. E., & Olins, A. L. (1971) *J. Mol. Biol.* 57, 437.
- Olins, D. E., Bryan, P. N., Harrington, R. E., Hill, W. E., & Olins, A. L. (1977) *Nucleic Acids Res.* 4, 1911.
- Poon, N. H., & Seligy, V. L. (1980) *Exp. Cell Res.* 128, 333.
- Privalov, P. L., & Khechinashvili, N. N. (1974) *J. Mol. Biol.* 86, 665.
- Ramsay, G., & Freire, E. (1990) *Biochemistry* 29, 8677.
- Roark, E. E., Goeghegan, T. E., Keller, G. H., Matter, K. V., & Engle, R. C. (1976) *Biochemistry* 15, 3019.
- Rubin, R. L., & Moudrianakis, E. N. (1972) *J. Mol. Biol.* 67, 361.
- Shih, T. Y., & Bonner, J. (1970) *J. Mol. Biol.* 48, 469.
- Shih, T. Y., & Fasman, G. D. (1971) *Biochemistry* 10, 1675.
- Simpson, R. T. (1979) *J. Biol. Chem.* 254, 10123.
- Spiker, S., & Isenberg, I. (1977) *Biochemistry* 16, 1819.
- Thompson, K. S., Vinson, C. R., & Freire, E. (1993) *Biochemistry* 32, 5491.
- van Holde, K. E. (1989) in *Chromatin*, pp 16–30 and 219–288, Springer-Verlag, New York.
- Weischet, W. O., Tatchell, K., van Holde, K. E., & Klump, H. (1979) *Nucleic Acids Res.* 5, 139.

BI950062F